# Image Resolution in Liquid Development for Electrophotography

**I. Chen**▲

*Wilson Center for Research and Technology, Xerox Corporation, Webster, New York*

The charge transport model of liquid immersion development (LID) is extended for consideration of line-pair images. The transfer of modulation from the image-wise charge distribution on the photoreceptor surface to the developed toner mass distribution is examined as a function of line-width. The line-width dependence of the modulation transfer is found to be weaker than that previously expected for electrostatic images, even at line-widths of small multiples of the receptor thickness. This indicates a favorable image resolution for LID that can be attributed to a new reason that is inherent in the electrophoretic development process, and is independent of the toner size or the development gap size.

Journal of Imaging Science and Technology 43: 270–273 (1999)

## Introduction

Development of electrostatic images with toners dispersed in non-polar liquids, i.e., liquid immersion development (LID), has been generally perceived to possess the potential of achieving the high image resolution demanded by high quality color prints due to the smaller toner size (~1 μm) and the feasibility of narrower development gap (<100 μm).[1,2] Although laboratory models as well as commercial printers based on LID[3,4] have demonstrated high quality color prints as expected, there is no quantitative analysis of the attributes responsible for the high image quality. Recent mathematical models of LID in the literature,[5–7] though quite extensive in taking into consideration the space-charge effects, are all limited to the treatment of solid-area images, and hence, do not provide information on the image resolution power associated with the electrophoretic development process. In this article, the charge transport model of LID is extended for consideration of line-pair images. The transfer of modulation from the image-wise charge distribution on the photoreceptor surface to the developed toner mass distribution is examined as a function of line-width. The line-width dependence of the modulation transfer is found to be weaker than that previously expected for electrostatic images, even at line-widths of small multiples of the receptor thickness. This indicates that there is a new reason for a favorable image resolution for LID, that is *inherent in the electrophoretic development process*, and is independent of the previously suggested processes, namely, the small toner size or the small development gap.

The mathematical procedure for calculating the toner deposition in LID of line-pair images is described in the next section. This is followed by the presentation and discussion of the major numerical results. A comparison with previous treatments of image resolution for electrostatic images suggests the physical reason for the favorable image resolution.

## Mathematical Procedure

As in the previous work,[6] the development zone is represented by the plane-parallel geometry shown in Fig. 1. The electrophoresis in the liquid developer (or ink), $0 \le z \le L_i$, is described by the continuity equations for the charge densities $\rho(x, z)$,

$$\partial\rho/\partial t = \pm \nabla(\mu\rho\mathbf{E}) \tag{1}$$

where $\rho$ stands for the charge densities of toners $\rho_t$ and counter-ions $\rho_p$, and $\mu$ stands for the corresponding mobilities $\mu_t$ and $\mu_p$. In inks of practical interest, the density of co-ions is usually so small that it is neglected for simplicity in this discussion. Without loss of generality, the toners are assumed to be negatively- and the counter-ions positively-charged. The field $\mathbf{E}(x, z)$ can be calculated from the potential $V(x, z)$, that can be obtained from the solution of Poisson's equation,

$$\nabla\mathbf{E} = -\nabla^2 V = (\rho_t + \rho_p)/\varepsilon_i \tag{2}$$

with the boundary condition that the discontinuity in the normal ($z$) component of electric displacements at $z = 0$ is equal to the charge density $Q_s(x)$ at the receptor surface,

$$\varepsilon_i E_{iz}(x, 0) - \varepsilon_r E_{rz}(x, 0) = Q_s(x) \tag{3}$$

where $\varepsilon_i$ and $\varepsilon_r$ are the permittivities, and $E_{iz}$ and $E_{rz}$ are the normal components of fields in the ink and receptor, respectively. The receptor is assumed to be space-charge-free during the development. Other boundary conditions are that the receptor is grounded at the substrate ($z = -L_r$), i.e., $V(x, -L_r) = 0$, and that a bias voltage $V_b$ is applied at the development electrode at $z = L_i$,

Original manuscript received February 12, 1998

▲ IS&T Member

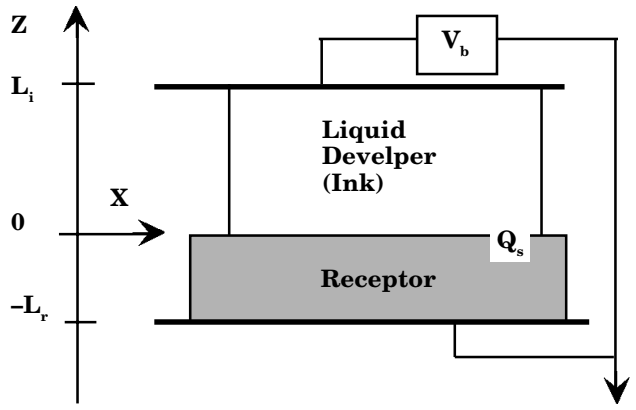


**Figure 1.** Schematic geometry and coordinate system for the mathematical model of liquid immersion development.

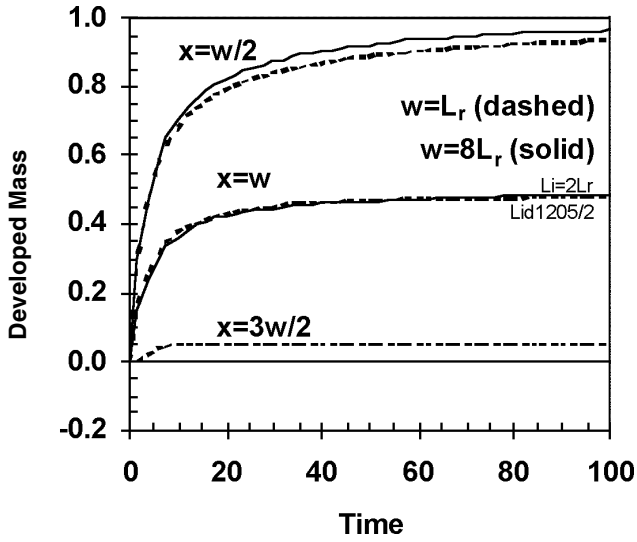


**Figure 2.** Time evolution of developed mass/area, $M(x,t)$, calculated from the deposit toner charge $Q_t(x, t)$, at three positions in a sinusoidal line-pair, the peak ($x = w/2$), the node ($x = w$) and the valley ($x = 3w/2$), for two line-widths $w$. The normalized units for mass/area, $M_o \equiv -Q_o/q_m$, and time, $t_o \equiv \varepsilon_i/\mu_t\rho_o$, are defined in the text.

i.e., $V(x, L_i) = V_b$. The initial conditions are that both the toner and the counter-ion charge distributions in the ink are uniform, having the values $-\rho_t(x, z) = \rho_p(x, z) = \rho_o$.

The toner deposition results from the arrival of toner current $J_{zt}(0)$ at the receptor surface. This is represented by the time rate of change of toner charge $Q_t(x, t)$ at the surface $z = 0$ as,

$$\partial Q_t(x, t)/\partial t = -J_{zt}(0) = -[\mu_t\rho_t E_z]_{z=0} \quad (4)$$

with the initial value, $Q_t(x, 0) = 0$. The initial charge distribution at the receptor surface is that of the line-pair image, given by a sinusoidal function of line-width $w$, (i.e., period $2w$), and amplitude $Q_o$,

$$Q_s(x, 0) = (Q_o/2)[1 + \sin(\pi x/w)] \quad (5)$$

where the charge polarity is assumed to be positive, $Q_o > 0$, to be consistent with the assumption of negative toners. It is assumed that toners and/or counter-ions arriving at the receptor surface come in close contact with, and modify, the surface charge density $Q_s$ according to the time rate of change,

$$\partial Q_s(x, t)/\partial t = J_{zp}(0) - J_{zt}(0) = [\mu_p\rho_p E_z]_{z=0} - [\mu_t\rho_t E_z]_{z=0} \quad (6)$$

Because the ink layer is neutral and space-charge-free at $t = 0$, Eq. 2 reduces to Laplace equation whose solution can be expressed in a closed form as,[1,8]

$$V(x, z) = U_0(z) + U_1(z)\sin(\pi x/w) \quad (7)$$

where, in the receptor, $-L_r \le z \le 0$,

$$U_0(z) = (V_b + Q_o D_i/2)(D_r + z/\varepsilon_r)/(D_r + D_i) \quad (8a)$$

$$U_1(z) = (wQ_o/2\pi)\sinh[\pi(L_r + z)/w]/[\varepsilon_r\cosh(\pi L_r/w) + \varepsilon_i\coth(\pi L_i/w)\sinh(\pi L_r/w)] \quad (9a)$$

and in the ink, $0 \le z \le L_i$.

$$U_0(z) = [(V_b + Q_o D_i/2)D_r + (V_b - Q_o D_r/2)z/\varepsilon_i]/(D_r + D_i) \quad (8b)$$

$$U_1(z) = (wQ_o/2\pi)\sinh[\pi(L_i - z)/w]/[\varepsilon_r\coth(\pi L_r/w)\sinh(\pi L_i/w) + \varepsilon_i\cosh(\pi L_i/w)] \quad (9b)$$

with $D_r = L_r/\varepsilon_r$, and $D_i = L_i/\varepsilon_i$.

Using the above initial values and time derivatives, the time evolution of the charge distributions can be calculated numerically. A feature that differs from the previous case of solid-area images is that the two-dimensional Poisson equation has to be solved by the finite difference method at each time interval $t > 0$.

## Results and Discussion

For a constant toner charge-to-mass ratio $q_m$, the distribution of developed toner mass, $M(x, t)$ can be obtained from the total toner charge at the receptor surface, $Q_t(x,t)$ of Eq. 4, as

$$M(x, t) = Q_t(x, t)/q_m \quad (10)$$

Figure 2 shows the time evolution of $M(x, t)$ at three positions in a line-pair: the peak (at the center of *on* line, $x = w/2$), the node (at the geometrical border between *on* and *off* lines, $x = w$) and the valley (at the center of *off* line, $x = 3w/2$), for two line-widths $w = 1$ and 8, in multiples of the receptor thickness $L_r$. The ink layer thickness is $L_i = 2L_r$; the permittivities of ink and receptor are equal, $\varepsilon_i = \varepsilon_r$; the toner and counter-ion mobilities are equal, $\mu_t = \mu_p$. The initial toner (or counter-ion) charge density is $\rho_o = Q_o/L_r$. The developed mass $M$ is given in units of $M_o \equiv -Q_o/q_m$ where $Q_o$ is the initial charge amplitude introduced in Eq. 5. The abscissa, time, is in units of $t_o \equiv \varepsilon_i/\mu_t\rho_o$ (which can be recognized as the dielectric relaxation time of the ink). For typical values of $L_r = 25$ μm, $q_m = -250$ μC/g, $Q_o = 50$ nC/cm², $\varepsilon_i = 2 \times 10^{-13}$ F/cm, and $\mu_t = 10^{-4}$ cm²/Vs, the units have values of $M_o = 0.2$ mg/cm² and $t_o = 10^{-4}$ s.

The development is seen to approach saturation in about 100 $t_o$. The asymptotic spatial distributions of $M(x, t)$ for the above two line-pair images are shown in Fig. 3. For comparison, the initial surface charge distribution, $Q_s(x,0)$ of Eq. 5, is also shown (in units of $Q_o$).

The effects of reduced line-width can be seen in Fig. 2 as the slightly slower build up of the developed mass at the peak ($x = w/2$) and a larger deposition at the valley ($x = 3w/2$). The incomplete neutralization, seen in Fig. 3 near the peak, is a consequence of space-charge-limited transport, and the deposition near the valley, (especially for the narrower line), is caused by the fringe fields. The combined effects lead to a smaller developed

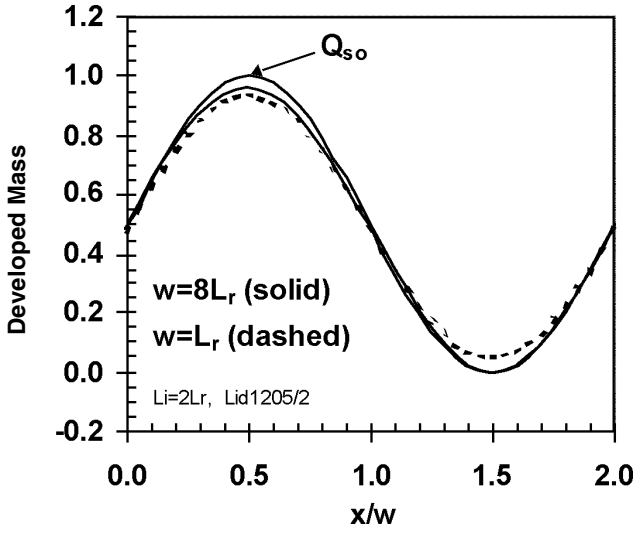


**Figure 3.** Spatial distributions of the developed mass/area, $M(x, t)$ at $t = 100\ t_o$, for two line-widths $w = 8$ and 1 in multiples of the receptor thickness $L_r$. The initial surface charge distribution $Q_{so} = Q_s(x,0)$ is also shown for comparison.

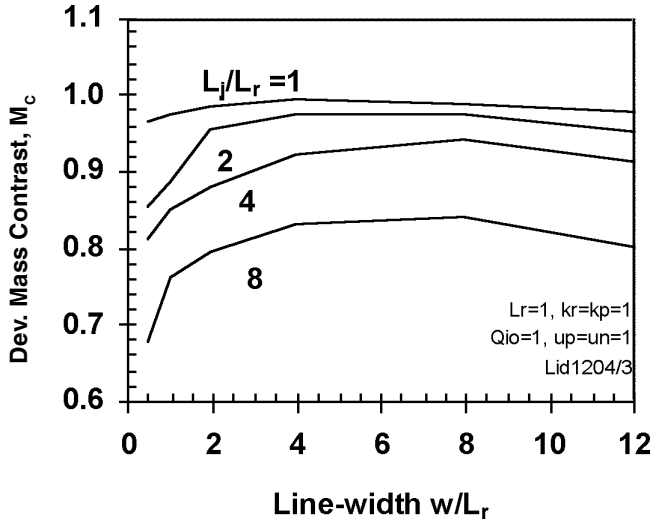


**Figure 4.** Developed mass contrast, $M_C(w)$ versus line-width $w$, for four values of ink-layer thickness $L_i$. $w$ and $L_i$ are in units of the receptor thickness $L_r$. The contrast is normalized to the maximum value $Q_o/q_m$.

mass contrast $M_C$ for the narrower line, where $M_C$ is defined as the difference in the asymptotic values, $M(x, t_\infty)$, at the peak and the valley,

$$M_C(w) \equiv M(w/2, t_\infty) - M(3w/2, t_\infty) \qquad (11)$$

Figure 4 shows the developed mass contrast $M_C$ (in units of $-Q_o/q_m$) as a function of line-width, for four values of ink layer thickness, $L_i$. The change of $M_C$ with line-width is seen to increase slightly as the ink layer thickness increases from $L_i = 1$, to $8L_r$. Similar results are obtained with other values of parameters within the range of practical interest (e.g., with $\mu_i \neq \mu_p$ and $\varepsilon_i \neq \varepsilon_r$). The decrease of contrast with decreasing line-width represents the loss of modulation transfer, resulting in failure to resolve fine lines. The loss of modulation transfer at small line-widths is common in many imaging processes, and can occur in various stages—in exposure, development and/or transfer. A striking observation from Fig. 4 is the smallness of this resolution loss compared to what is previously expected for electrostatic imaging process.[1,2]

Although many different methods have been used to develop electrostatic latent images,[2,9,10] the image resolution has only been discussed by examining how well the modulation in the image-wise charge distribution is retained in the surface voltage or field distributions.[1,2] The developed mass distribution is assumed to be proportional to the surface voltage or field from the image-wise charge distribution. Thus, for example, for the sinusoidal line charge pattern $Q_s(x, 0)$ of Eq. 5, the surface voltage $V(x, 0)$, and the normal component of field $E_z(x, z)$ can be calculated from Eqs. 7, 8(b), and 9(b). The mass contrast $M_V$ that is proportional to the modulation of the surface voltage would be,

$$M_V(w) \propto V(w/2, 0) - V(3w/2, 0) = (wQ_o/\pi)/[\varepsilon_r \coth(\pi L_r/w) + \varepsilon_d \coth(\pi L_d/w)] \qquad (12)$$

and the mass contrast that is based on the modulation of the normal field at $z$ is,

$$M_E(w) \propto E_z(w/2, z) - E_z(3w/2, z) = Q_o \cosh[\pi(L_d - z)/w]/[\varepsilon_r \coth(\pi L_r/w)\sinh(\pi L_d/w) + \varepsilon_d \cosh(\pi L_d/w)] \qquad (13)$$

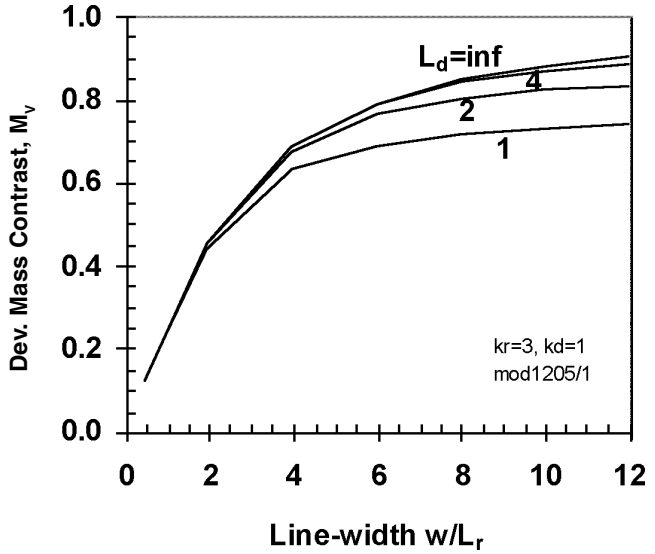


**Figure 5.** Developed mass contrast based on surface voltage, $M_V$, Eq. 12, versus line-width $w$, calculated for four values of development gap $L_d$. $w$ and $L_d$ are in units of the receptor thickness $L_r$, and $M_V$ is normalized to its maximum as unity.

where the subscript $i$ for the ink layer is replaced by $d$ for the development gap. The line-width dependence of $M_V$ and $M_E$, for the geometrical conditions similar to that of Fig. 4 are shown in Figs. 5 and 6, respectively, and discussed below. The contrasts are in units normalized to the maximum as unity (i.e., voltage modulation in units of $Q_oL_r/\varepsilon_r$, and the field modulation in units of $Q_o/\varepsilon_r$).

The decrease in the voltage-based mass contrast $M_V$ due to the line-width reduction is seen in Fig. 5 to be much more pronounced than that for the mass contrast $M_C$ shown in Fig. 4. The curves corresponding to the case of development gap $L_i$ or $L_d = 2L_r$, from each of the three figures, are reproduced for comparison in Fig. 7. The variation of the field-based mass contrast $M_E$ calculated with the field at $z = 0.2L_r$ above the receptor surface, as shown in Fig. 6, has an appearance different from that of $M_V$ in Fig. 5. For the development gap

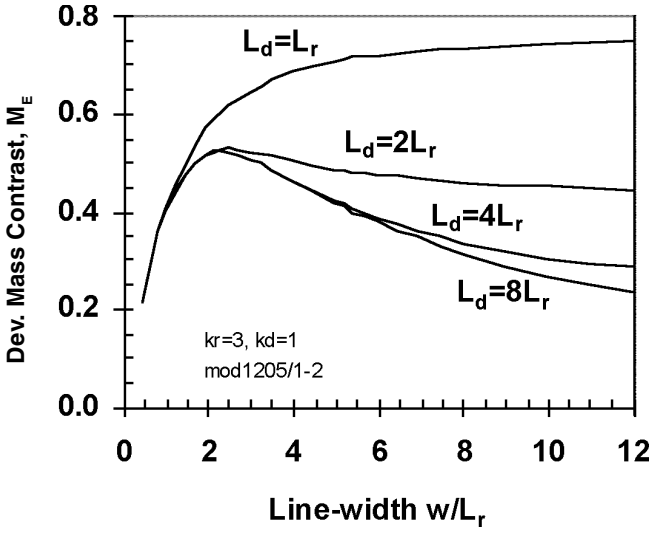


**Figure 6.** Developed mass contrast based on normal field, $M_E$, Eq. 13, versus line-width $w$, calculated at a distance $z = 0.2$ above the surface, for four values of development gap $L_d$. $w$, $z$ and $L_d$ are in units of the receptor thickness $L_r$, and $M_E$ is normalized to its maximum as unity.

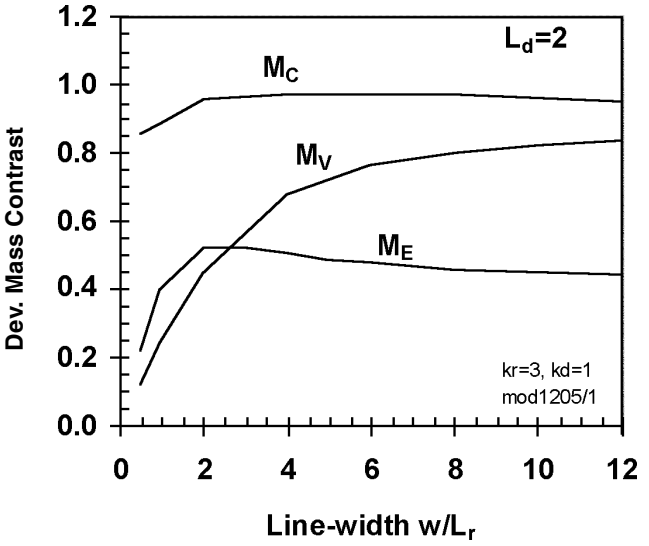


**Figure 7.** Comparison of developed mass contrasts calculated from deposit toner charge $M_C$, Eq. 11, from voltage modulation $M_V$, Eq. 12, and from field modulation $M_E$, Eq. 13, for the case of development gap $L_i$ or $L_d = 2L_r$, (i.e., the reproduction of one curve each from Figs. 4, 5 and 6).

greater than the receptor thickness, $L_d > L_r$, a maximum in contrast $M_E$ appears at a line-width $w \approx 2L_r$. This is the well-known account for the poor development of solid-area as well as very fine line electrostatic images with a large development gap (e.g., cascade development). Furthermore, contrary to the case of voltage-based $M_V$, the field-based $M_E$ is larger for the smaller development gap (Fig. 6). In fact, based on the latter feature, Schaffert has predicted a higher resolution of LID than dry-toner development because of the feasibility of smaller gap in LID.[1,2]

Returning to Fig. 4, the similar increase of contrast with decreasing gap (or ink layer thickness) is seen for the mass contrast $M_C$, which is calculated directly from the electrophoretic motion of charged species. In other words, the LID mass contrast $M_C$ is more similar to the field-based contrast $M_E$, rather than to the voltage-based contrast $M_V$. This suggests a physical reason for the weaker line-width dependence of $M_C$, shown in Figs. 4 and 7, namely, the importance of local field variation due to the space-charge-perturbed electrophoretic motion in LID. It should be noted that the contrasts shown in Figs. 5 and 6 are calculated with the voltage and the field in a space-charge-free development gap, from the solutions of Laplace equation, Eqs. 7, 8(b), and 9(b), based on the initial image-wise charge distribution. However, the gap is not space-charge-free during most of LID time. The fields used in the calculation of curves in Fig. 4 are the self-consistent fields from the solutions of Poisson's equation, based on the instantaneous distributions of charges in the gap (or ink) and the neutralized image-wise charge on the receptor surface.

It is expected that image resolution can be described by the voltage-based mass contrast $M_V$, if the toner deposition is generation-limited. That is, the electrostatic force from the image-wise charge is used mostly to create free toners, which arrive at the receptor surface almost instantaneously because of the high mobility, e.g., in the dry media. On the other hand, the toner deposition in LID is transport- and space-charge-limited, because of the large amounts of toner and counter-ion charge that move simultaneously in the more viscous and lower mobility liquid media. The local field that determines the transport is influenced by the local charge densities (of toners and counter-ions in the gap) as much as by the charge on the receptor.

## Summary and Conclusions

The charge transport model of liquid immersion development is extended and applied to line-pair images of various line-widths. The developed mass distributions in the direction perpendicular to the line are calculated from the toner charge deposited on the receptor, and the peak-to-valley contrasts are investigated as a function of line-width. The decrease of modulation transfer with the line-width is found to be much less serious than that previously expected for electrostatic imaging. This indicates a favorable image resolution which can be attributed to a new reason *inherent* in electrophoretic motions of toners and counter-ions in LID, hence, non-existant in dry powder development. The consideration of the contributions from toner and counter-ion space charges and the time-varying receptor surface charge to the electric fields that drive the development, is suggested as the physical reason for the difference. ▲

**Acknowledgment.** The author wishes to thank Dr. J. Mort for valuable discussions on the subject of this work.

## References

1. R. M. Schaffert, *Photogr. Sci. Eng.* **6,** 197 (1962).
2. R. M. Schaffert, *Electrophotography*, Focal Press, London, 1975.
3. M. Omodani, M. Fujita, M. Ozawa, and M. Ohta, *IS&T's NIP13: Intl. Conference on Digital Printing Technologies*, IS&T, Springfield, VA, 1997, p. 820
4. Y. Niv, *IS&T's 10th Intl. Congress on Advances in Non-Impact Printing Technol.*, IS&T, Springfield, VA, 1994, p. 196
5. G. Bartscher and J. Breithaupt, *J. Imaging Sci. Technol.* **40,** 441 (1996), and references therein.
6. I. Chen, *J. Imaging Sci. Technol.* **39,** 473 (1995).
7. I. Chen, J. Mort, M. A. Machonkin, J. R. Larson, and F. Bonsignore, *J. Appl. Phys.* **80,** 6796, (1996)
8. I. Chen, *Photogr. Sci. Eng.* **26,** 153 (1982).
9. E. M. Williams, *The Physics and Technology of Xerographic Processes*, John Wiley and Sons, New York, 1984.
10. L. B. Schein, *Electrophotography and Development Physics*, Springer-Verlag, Berlin, 1988.